JOURNAL OF MATERIALS SCIENCE 28 (1993) 2040–2048

Microstructure and mechanical properties of Fe_3Al alloys with chromium

J. R. KNIBLOE, R. N. WRIGHT, C. L. TRYBUS
Idaho National Engineering Laboratory, Idaho Falls, ID 83415, USA
V. K. SIKKA
Oak Ridge National Laboratory, Oak Ridge, TN, USA

Alloys based on Fe_3Al have an equilibrium DO_3 structure at low temperatures and transform to a B2 structure above about 550 °C. The influence of different rates of quenching from the B2 region to room temperature and of subsequent heat treatments on the microstructure and mechanical properties of powder metallurgy (P/M) alloys with two different chromium contents have been examined. Optimizing the processing to maximize the amount of B2 order, without eliminating dislocations that enhance both strength and ductility, yields room-temperature ductility approaching 20%, although the fracture mode is primarily brittle cleavage. The B2 structure generally has lower flow stress than the DO_3 structure because of its lower strain-hardening rate, although B2 order actually has higher yield strength when the structure is free of dislocations. Increasing the chromium content from 2% to 5% has little effect on ductility, although the 2% Cr alloys generally have higher yield strengths and larger order parameters.

1. Introduction

Fe_3Al-based alloys exhibit good oxidation and sulphidation resistance as well as excellent resistance to abrasive wear and erosion [1], but until recently interest in these alloys has been limited because of their low room-temperature ductility. Liu *et al.* [2–4] and others [5, 6] have recently discovered that the limited ductility of iron aluminides is largely the result of environmental embrittlement. Tensile elongations of specimens tested in air or H_2O + argon are significantly less than those of specimens tested in dry oxygen [4], vacuum [6] or even hydrogen + argon [2, 3]. This is attributed to embrittlement by atomic hydrogen generated by a reaction with water vapour, similar to that found in many aluminium alloys. Tensile testing under various conditions of controlled pH and electrochemical potential indicate that atomic hydrogen is particularly detrimental to ductility, but that non-dissociated water molecules also cause embrittlement [5].

Fe_3Al alloys with higher strength and improved ductility have resulted from increased understanding of alloying and thermomechanical processing effects [7, 8]. Chromium is added principally to improve the room-temperature ductility [7, 8], while other alloying elements such as niobium, molybdenum and silicon appear to improve the elevated temperature strength but are deleterious to room-temperature ductility [9–11]. Warm working the material to create a high defect density at room temperature and appropriate heat treatments are thought to markedly increase the room-temperature ductility [12]. Powder metallurgy (P/M) methods offer the potential of a refined grain size in the final product, thus increasing the strength without significantly reducing the ductility.

A portion of the Fe–Al phase diagram is shown in Fig. 1. Compositions with stoichiometry of approximately 3 iron to 1 aluminium have three possible crystal structures. Above about 900 °C, a solid solution of the two elements on a bcc lattice is the equilibrium structure. Two ordered phases exist at lower temperatures. The FeAl phase field shown in Fig. 1 is present above a critical temperature of about 550 °C and has the B2 structure. For compositions with an equiatomic stoichiometry the B2 structure has one type of atom at the corner sites of a cube and the other type at the centre; however, for Fe_3Al stoichiometry, iron atoms occupy all of one type of site, and the other sites are occupied by iron atoms and aluminium atoms with equal probability. Below the critical temperature, DO_3 is the equilibrium structure (labelled Fe_3Al in Fig. 1). Fig. 2 illustrates the DO_3 structure. For both B2 and DO_3 order it is assumed that chromium, the alloying element used in this study, occupies iron and aluminium sites with equal probability [7]. The critical temperature can be altered substantially by the addition of certain alloying elements, although chromium has little effect [7].

Only by very rapid cooling can disordered phase be preserved at room temperature. However, in chromium-containing alloys, a structure of primarily B2 phase can easily be obtained by quenching from above the critical temperature, indicating that the $B2 \leftrightharpoons DO_3$

0022–2461

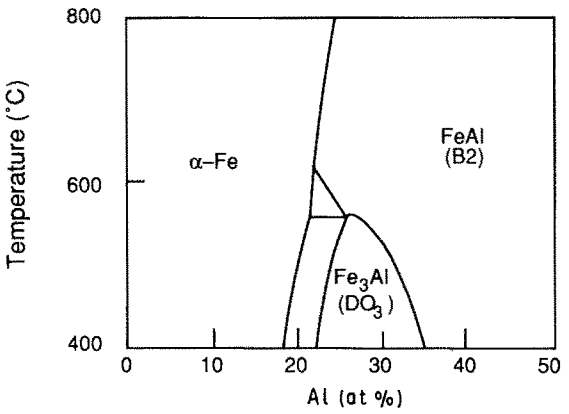

Figure 1 Iron-rich portion of the Fe–Al equilibrium phase diagram.

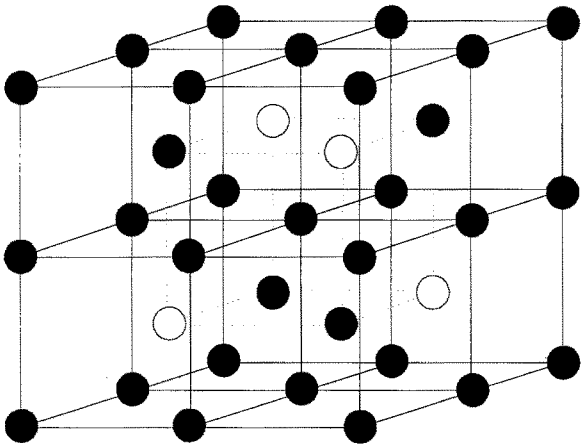

Figure 2 The DO_3 crystal structure. Iron atoms occupy all sites marked (●); aluminium atoms occupy the remaining sites, denoted (○).

transformation is sluggish [13, 14]. By quenching from different temperatures and with different media, the relative volume fractions of the two ordered phases can be controlled. This is not the case for binary iron aluminides that have a rapid $B2 \leftrightharpoons DO_3$ transformation [15, 16]. The amount of each type of order can be described by the Bragg–Williams long-range order parameter, S, defined as

$$S = \frac{(r_A - f_A)}{(1 - f_A)} \quad (1)$$

where r_A is the fraction of A sites occupied by the "right" atoms and f_A is the fraction of A atoms in the alloy. An S of 1.0 indicates perfect order of a certain type, and values less than 1.0 indicate a departure of the bulk sample from this perfect order. This parameter is determined by measuring the integrated intensity of the X-ray diffraction (XRD) peaks and comparing the measured values with calculated values for perfect order of the different phases.

In the present work, the effect of different heat treatments on the microstructure of two chromium-containing Fe_3Al alloys was examined by the use of XRD, transmission electron microscopy and optical metallography. The mechanical properties resulting from the various structures have been determined by room-temperature tensile testing of extruded and hot-rolled materials produced by P/M processing.

2. Experimental procedure

Two batches of powder with stoichiometries designed to yield Fe_3Al containing nominally 2% or 5% Cr by weight were produced by inert gas atomization with argon. The alloys were melted in zirconia crucibles prior to atomization; there was no indication of gross chemical interaction between the melt and the ceramic material.

The powders were canned in mild steel, evacuated and hot extruded at 1000 °C to an area reduction ratio of 9:1. The as-extruded structure was examined using standard optical metallography techniques. Round tensile bars were machined by centreless grinding from a portion of the extrusions. Tensile bars were tested in both the as-extruded and heat-treated conditions as described in Table I. A portion of the 5% Cr alloy extrusion was squared, annealed for 1 h at 1100 °C, clad in mild steel, and rolled to 10% and 30% reductions in thickness at 650 °C to introduce two different densities of defects. Round tensile specimens machined from these materials were tested in the as-rolled condition and after heat treatment as outlined in Table I.

After removing the steel can, another portion of each alloy extrusion was forged at 1000 °C to 8.6 mm thick and then rolled at 800 °C to sheet approximately 2.54 mm thick. The sheet was finish rolled at 650 °C to 0.76 mm. Tensile specimens were punched from the sheet and heat treated at temperatures from 700–850 °C before quenching in oil or air. All tensile testing of these punched sheet specimens was performed at a strain rate of $3.3 \times 10^{-3}\ s^{-1}$. Three additional rolled specimens were cut from the 2% Cr sheet before heat treating, carefully polished, and tensile tested at room temperature at a strain rate of $6.6 \times 10^{-4}\ s^{-1}$. The heat treatments for these samples were designed to result in varying amounts of the DO_3 ordered phase. The heat treatments for all sheet specimens described above are summarized in Table I.

After testing, the fracture surfaces of some of the samples were examined using SEM. The grip sections of the tensile bars were examined by standard optical metallography techniques to study the as-rolled structure and measure the grain size. The grain size was determined by the line intercept method. For a given specimen, four areas were photographed and three grain size measurements made on each area. Thin foils for TEM were prepared by electropolishing extruded transverse sections and by core drilling polished material from sheet short-transverse sections.

XRD was used to determine phases present and measure the order parameters in as-atomized powders, as-extruded material and heat-treated rolled specimens. Order parameters of the powder samples were determined by measuring the DO_3, B2 and fundamental peaks that occur at the lowest diffraction angle. Samples from the grips of tensile specimens were repeatedly etched and lightly repolished to remove any flowed metal on the surface that might affect the

TABLE I Summary of tensile specimens

Specimens machined from extruded bar (2% and 5% Cr)
As-extruded
800 °C 1 h, OQ, cleaned with acetone
1100 °C 1 h, FC to 750° C 1 h, OQ, cleaned with acetone
1100 °C 1 h, FC to 750 °C 1 h, cleaned with acetone, OQ, 500 °C 48 h, FC
Specimens machined from bar, annealed 1100 °C 1 h, and rolled (5% Cr only)
10% reduction in thickness, as-rolled
10% reduction in thickness, 750 °C 1 h, OQ, cleaned with acetone
30% reduction in thickness, as-rolled
30% reduction in thickness, 750 °C 1 h, OQ, cleaned with acetone
Specimens punched from rolled sheet after stress relief of 700 °C 1 h, OQ (2% and 5% Cr)
700 °C 1 h, AC + OQ[a]
750 °C 1 h, AC + OQ[a]
800 °C 1 h, AC + OQ[a]
850 °C 1 h, AC + OQ[a]
Specimens machined from rolled sheet (2% Cr only)
700 °C 1 h, OQ, cleaned with acetone
700 °C 1 h, FC to 400 °C 24 h, OQ, cleaned with acetone
700 °C 1 h, FC to 500 °C 24 h, OQ, cleaned with acetone

AC, air cooled; FC, furnace cooled; OQ, oil quenched.
[a] One specimen was air cooled and one oil quenched.

shape of the diffraction peaks. Because significant preferred orientation from rolling and/or extrusion was detected in the rolled specimens, diffraction peaks of the same {1 1 1} family were selected for the order parameter measurements of the consolidated material. Diffraction step scans were done for each sample over regions where {1 1 1} peaks from each of the three possible structures occur. The order parameters, S, were calculated according to

$$\frac{I_{\text{super}}}{I_{\text{fundamental}}} = \frac{K|SF_{\text{super}}|^2}{|F_{\text{fundamental}}|_2} \quad (2)$$

where I is the integrated intensity of the measured peaks, and F is the structure factor calculated for the peaks. K is a constant determined by the Lorentz polarization factors, temperature corrections, and multiplicity factors of the peaks.

3. Results and discussion

The atomized powders of both compositions were generally spherical with a predominantly dendritic structure and had a mean particle size of approximately 40 μm. Chemical analyses of the two alloy powders are shown in Table II. The chromium contents, 1.94 and 4.63 wt %, are reasonably close to the target compositions of 2.0 and 5.0 wt %. The extrusions of both compositions were fully dense. The combination of large elongated grains and small equiaxed grains indicates that the material is partially recrystallized, with an average grain size of 11 and 16 μm for the 2% and 5% Cr alloys, respectively. Optical metallography showed no evidence of prior particle boundaries; however, TEM and electron energy loss spectroscopy (EELS) revealed aluminium oxide particles along the prior particle boundaries. A few small (60 nm diameter) ZrC particles were present, apparently from reaction of the melt with the ZrO_2 crucible. Some chromium-rich particles were also found in the 5% Cr alloy. Fig. 3 shows a typical microstructure taken in the plane of 5% Cr sheet that was hot rolled from the extrusion and subsequently heat treated at 700 °C. This structure also appears to be partially recrystallized and has an average grain diameter of 29 μm whereas the 2% Cr alloy has an average grain diameter of 33 μm. It has previously been reported that chromium has no effect on grain size in Fe_3Al [7]. The different cooling rate resulting from oil quenching rather than air cooling caused no difference in the structure that is apparent from optical metallography.

The tensile data for the sheet tensile specimens are presented in Figs 4 and 5. These P/M processed materials have finer grains and superior strength compared to similar traditional ingot metallurgy alloys

TABLE II Chemical analyses of Fe_3Al powders by X-ray fluorescence (wt %)

Powder	C	S	P	Si	Cr	Fe	Al
2% Cr	0.012	0.001	0.003	0.034	1.94	83.78	14.23
5% Cr	0.019	0.001	0.002	0.014	4.63	80.73	14.55

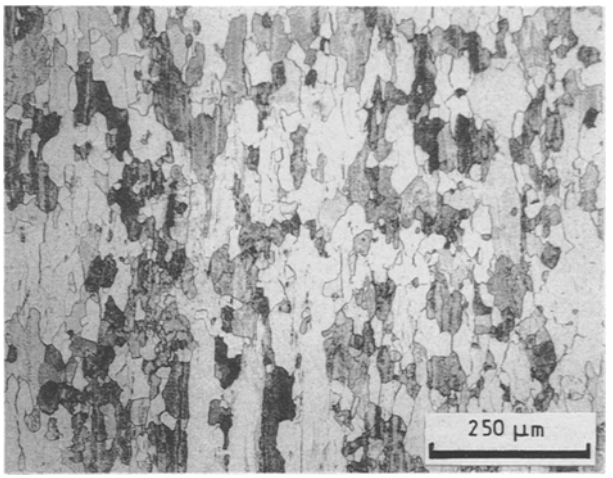

Figure 3 Microstructure of hot-rolled Fe_3Al with 5% Cr.

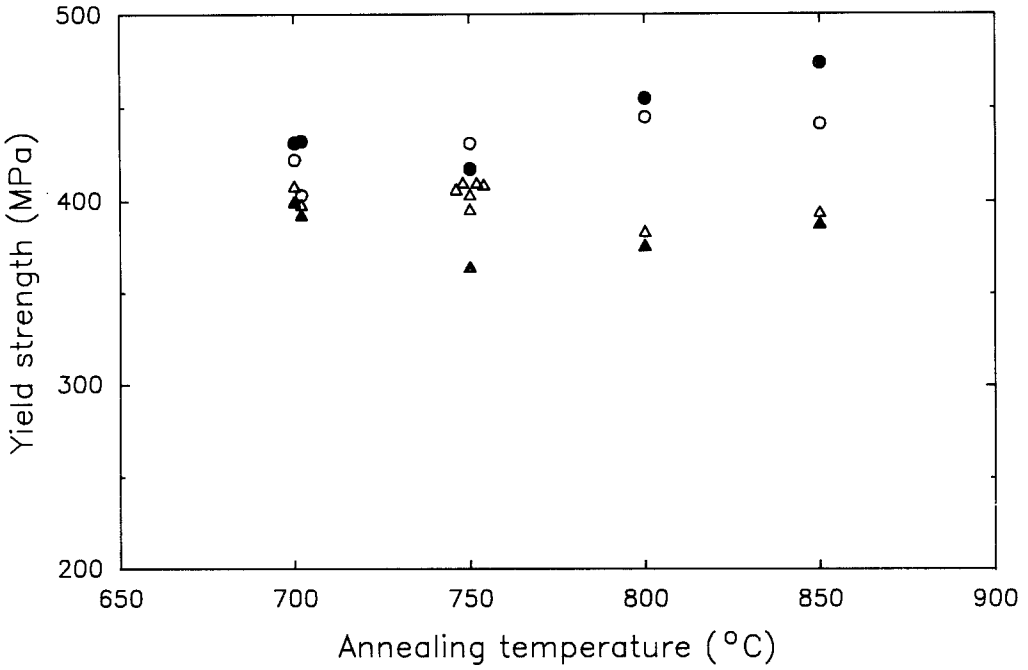

Figure 4 Yield strength as a function of annealing temperature for (○, ●) 2% and (△, ▲) 5% Cr sheet tensile specimens subjected to (○, △) oil quenching and (●, ▲) air cooling. Some data points are offset horizontally for clarity.

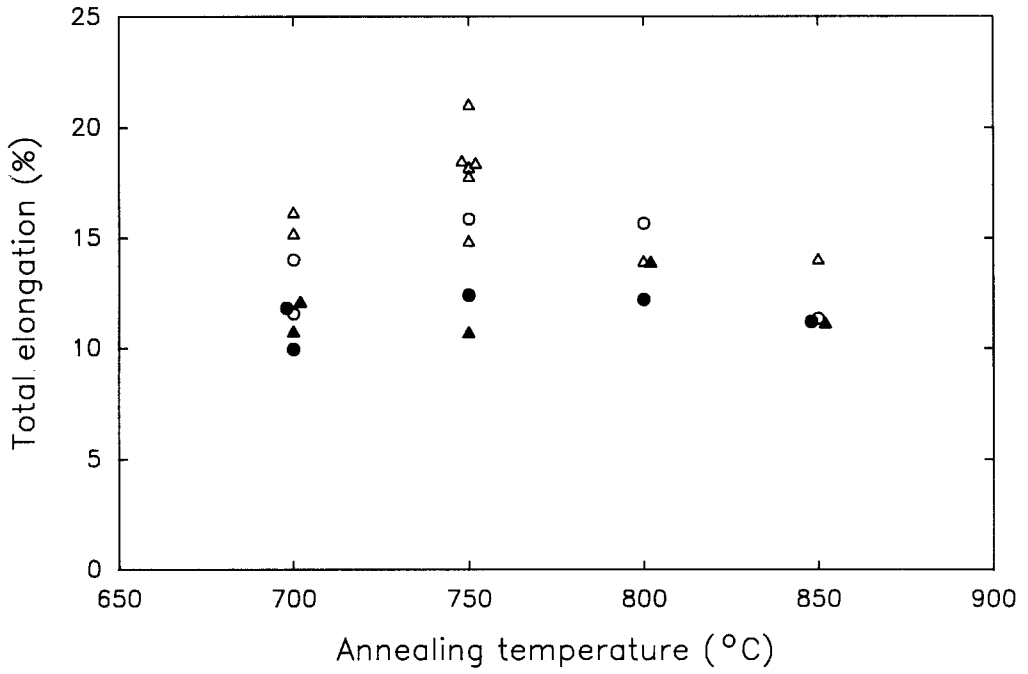

Figure 5 Total elongation as a function of annealing temperature for (○, ●) 2% and (△, ▲) 5% Cr sheet tensile specimens subjected to (○, △) oil quenching and (●, ▲) air cooling. Some data points are offset horizontally for clarity.

[17]. Five separate tensile tests for the 5% Cr alloy exposed to one of the heat treatments indicate good repeatability. The heat-treatment temperature has little effect on the tensile properties. However, the tensile specimens that were quenched into oil had better elongation than the air-cooled specimens of the same alloy and heat-treatment temperature in nearly every case. XRD of the quenched specimens indicates that no measurable DO_3 phase is present. In contrast, the air-cooled specimens have DO_3 order parameters of around 0.3 (see Table III). Previous studies have suggested that the presence of an oil film on the surface of the tensile specimens results in superior ductility by forming an effective barrier to hydrogen embrittlement [2, 9]. Although it is possible that this effect contributes to the differences evident in Fig. 5, it should be noted that all other tensile specimens in this study were cleaned in acetone before testing to remove any residual quenching oil. For a given heat treatment, the elongations of the 2% Cr alloy were generally about the same as those of the 5% Cr alloy although the yield strengths of the 2% Cr alloy may be

TABLE III Order parameters of selected samples

Description	2% Cr		5% Cr	
	S_{DO_3}	S_{B2}	S_{DO_3}	S_{B2}
As-atomized powder	0.25	0.13	0.24	0.18
As-extruded material	0.62	0.30	0.43	0.21
Rolled, 700 °C 1 h, oil quench, stamped, 700 °C 1 h, oil quench	0.00	0.23	0.00	0.23
Rolled, 700 °C 1 h, oil quench, stamped, 700 °C 1 h, air cool	0.29	0.29	0.20	0.21
Rolled, 700 °C 1 h, oil quench, stamped, 800 °C 1 h, oil quench	0.00	0.40	0.00	0.25
Rolled, 700 °C 1 h, oil quench, stamped, 800 °C 1 h, air cool	0.36	0.35	0.27	0.24
Rolled, cut, 700 °C 2 h, furnace cool to 400 °C and hold 24 h, oil quench	0.43	0.23	–	–
Rolled, cut, 700 °C 2 h, furnace cool to 500 °C and hold 24 h, oil quench	0.37	0.25	–	–

slightly higher. The higher strengths may be related to the amount of order, as the 2% Cr samples generally have somewhat higher order parameters than the 5% Cr samples. This variation in order with chromium content indicates that the presence of chromium may inhibit the DO_3 ordering process. This hypothesis is further supported by the fact that Fe_3Al without chromium transforms from B2 to DO_3 nearly instantaneously [15, 16], while the transformation in the chromium containing alloys in this study is quite sluggish as evinced by the suppression of the transformation by a simple oil quench from the B2 temperature regime.

Scanning electron microscopy of the fracture surfaces of several of the sheet specimens indicated primarily cleavage fracture. However, small areas of dimpled fracture were found in two quenched specimens that had total elongations greater than 15%. An example of this type of fracture is shown in Fig. 6. Energy dispersive spectroscopy (EDS) did not indicate any significant chemical differences between the cleavage and dimpled regions, or the presence of any particles, which might be an indication that the alumina, ZrC or chromium-rich particles mentioned above were detrimental. Inclusions in a binary Fe_3Al alloy studied previously [16] were also found not to cause brittle cleavage fracture. The brittle appearance of the fracture surfaces would suggest very little ductility; however, even the least ductile specimen had a total elongation of 10%. It has been hypothesized that these materials may have a finite cleavage strength resulting in brittle fracture after significant tensile elongation when strain hardening causes the flow stress to exceed the cleavage strength [16].

The trend of higher strength but lower ductility in samples of a given composition with higher DO_3 order is also found in extruded tensile specimens. The yield strengths and elongations of several extruded specimens are listed in Table IV. For both the 2% and 5% Cr alloy, extrusions that were quenched from above the critical temperature had ductilities that far

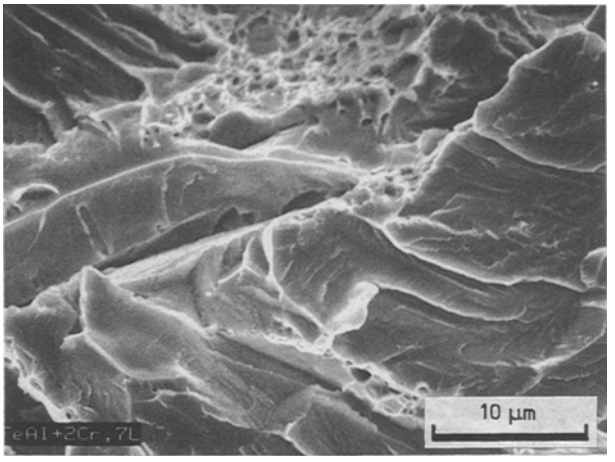

Figure 6 Scanning electron micrograph of fracture surface of Fe_3Al 2% Cr tensile bar.

exceeded the values for the as-extruded material. However, yield strengths of the as-extruded specimens were slightly higher than those of the heat-treated specimens. The as-extruded samples have very high DO_3 order parameters, although the high values were not anticipated based on the thermal history of the extrusions, whereas quenched material has no measurable DO_3 order. The as-extruded and quenched materials have nearly identical grain sizes for both alloys and the quenched samples were cleaned prior to testing, as mentioned above.

Specimens that were heat treated at 1100 °C to eliminate dislocations caused by the extrusion process prior to any ordering heat treatment had lower strength and ductility than specimens given similar ordering treatments without the 1100 °C anneal (see Table IV). Optical metallography indicates that this anneal results in an approximately three-fold increase in the grain size which may be the primary cause of the decreased strength and ductility. Fig. 7 shows a transmission electron micrograph of the essentially dislocation-free structure that results from the 1100 °C

TABLE IV Tensile properties of selected round specimens

Description[a]	2% Cr		5% Cr	
	Total elongation (%)	Yield strength (MPa)	Total elongation (%)	Yield strength (MPa)
as-extruded	11.7	615	6.1	503
extruded, quenched	15.6	548	16.1	490
annealed, quenched	12.2	494	11.8	358
annealed, low T hold	8.8	421	9.5	277
annealed, rolled 10%	–	–	8.8	490
annealed, rolled 30%	–	–	13.3	534
annealed, rolled 10%, quenched	–	–	13.8	399
annealed, rolled 30%, quenched	–	–	17.9	422

[a] Annealed = 1100 °C, 1 h to remove dislocations.
Quenched = oil quenched from 750–800 °C to maximize B2 order.
Low T hold = 500 °C, 48 h to maximize DO_3 order.
Rolled 10% = square bar rolled to 10% reduction in thickness.
Rolled 30% = square bar rolled to 30% reduction in thickness.

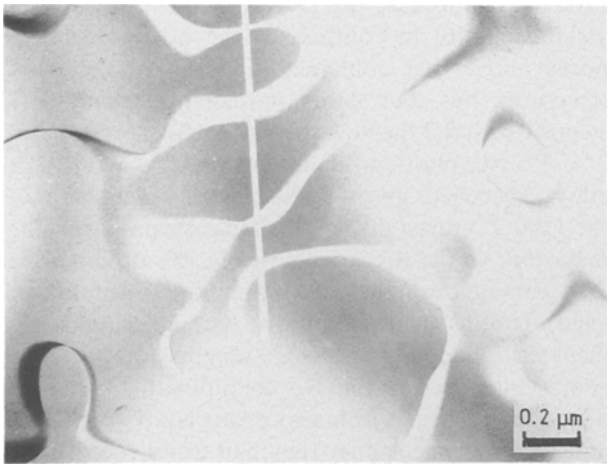

Figure 7 Transmission electron micrograph of 2% Cr material heat treated at 1100 °C for 1 h then given a heat treatment of 750 °C 1 h, oil quench followed by 500 °C 48 h, furnace cool to produce the DO_3 structure. The straight line is a slip anti-phase domain boundary.

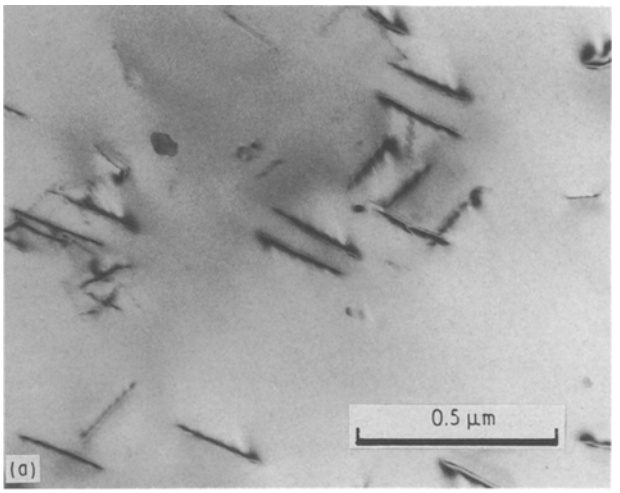

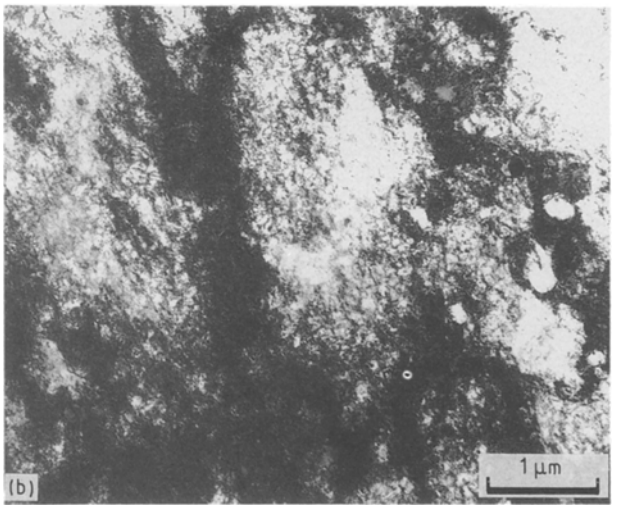

Figure 8 Fe_3Al + 5% Cr hot-rolled material (a) quenched from 750 °C after 1 h and (b) as-rolled.

anneal followed by a DO_3 ordering heat treatment. A lower dislocation density in the annealed material would also be expected to result in a lower yield strength. It has been suggested that dislocations are difficult to generate in Fe_3Al alloys [12], which could account for the lower ductility in the dislocation-free annealed samples. Alternatively, dislocations may serve as sinks for atomic hydrogen, inhibiting the hydrogen embrittlement phenomenon observed in these alloys. Despite the diminished mechanical properties, these dislocation-free specimens exhibit most of the same trends as other specimens, with the B2 specimens having higher ductility than the DO_3 specimens and the 2% Cr specimens having higher yield strengths than the 5% Cr samples for both types of order.

Strengths of extruded specimens quenched from 800 °C exceeded those of similarly heat-treated sheet specimens; however, they had similar ductility. This is at least partially a grain-size effect because the extruded material has a grain size about half that of the rolled material. There may be an additional contribution from substructure in the samples resulting from processing. TEM of rolled material after quenching from a heat treatment of 750 °C for 1 h (Fig. 8a) revealed a relatively low dislocation density compared to the as-rolled structure (Fig. 8b) resulting from

extensive recrystallization. TEM also showed a higher dislocation density in the as-rolled material than in the as-extruded material (Fig. 9). The larger amount of prior deformation in the rolled material could result in more extensive recrystallization in the rolled material heat treated at 750 °C than in the extruded material heat treated at 800 °C, which would account for the higher strength in the extruded material.

In a more controlled test of the combined influence of warm working and ordering, samples of the 5% Cr alloy were annealed for 1 h at 1100 °C prior to being rolled to 10% and 30% reductions in thickness at 650 °C to introduce two different densities of defects. TEM verified that the 30% reduction material has a higher dislocation density than the 10% reduction material, yet they have similar grain sizes of 51 and 49 μm, respectively. Because of the cladding, these samples are expected to have cooled slowly enough to result in some DO_3 order and an order parameter of 0.19 was measured in similarly processed material rolled to a 20% reduction in thickness. Additional samples were given a B2 ordering heat treatment prior to tensile testing that did not create a measurable difference in grain size. The higher defect density specimens had greater elongations and higher yield strengths in both the as-rolled and heat-treated conditions, and the B2 ordered samples had greater elongations but lower yield strengths for both thickness reductions (see Table IV). This clearly shows that both prior work and the B2 order condition enhance the room-temperature ductility.

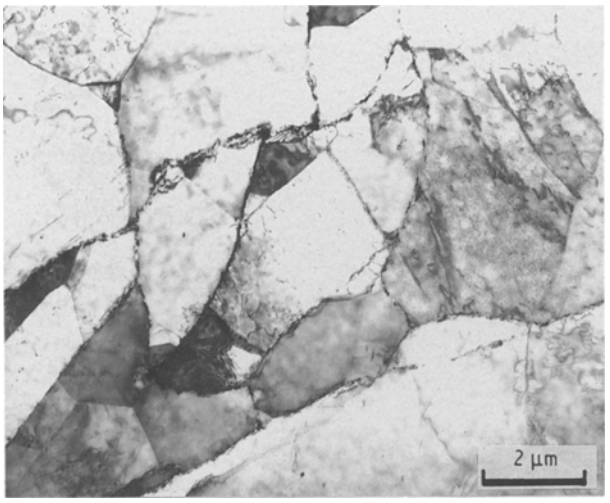

Figure 9 Transmission electron micrograph of typical as-extruded microstructure.

Fig. 10 shows the true stress–true plastic strain curves for samples of both alloys that received the ordering heat treatments after recrystallization at 1100 °C. In this case the DO_3 specimens have lower yield strengths, in contrast to the other specimens noted above that contained significant defect substructures, but they strain harden more, and consequently exceed the flow stress of the B2 specimens at 2%–3% true plastic strain for both the 2% and 5% Cr alloys. Specimens given the B2 heat treatment without the 1100 °C anneal displayed similar strain-hardening behaviour to the B2 samples in Fig. 10, although the flow curves are higher corresponding to the higher yield strengths mentioned above. It appears that specimens that had higher yield strengths for the DO_3 condition than for the B2 condition had residual dislocation densities from processing equivalent to the annealed specimens after they had experienced more than 3% plastic strain, so that the yield strengths are

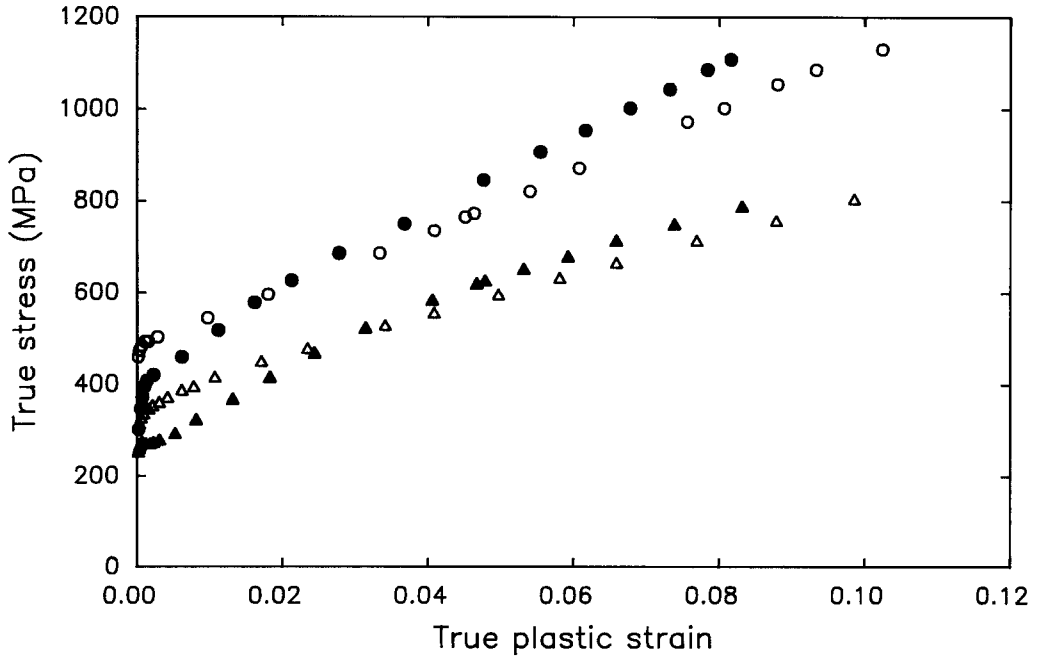

Figure 10 Flow curves for the (○, ●) 2% and (△, ▲) 5% Cr specimens annealed at 1100 °C to remove dislocation followed by (○, △) B2 and (●, ▲) DO_3 ordering heat treatments prior to tensile testing.

comparable to the greater flow stress of recrystallized DO_3 specimens in Fig. 10 once dislocations are generated and strain hardening has taken place.

The strain hardening rate, $d\sigma/d\varepsilon$, was determined as a function of plastic strain in the range of about 0.5%–10% for these specimens. Higher and lower strain regions were not considered in order to eliminate anomalous results created by the onset of necking, differences in ductility, and yield drops in some samples. Both sets of B2 specimens exhibit an essentially constant strain-hardening rate with the dislocation-free samples strain hardening at a slightly lower rate. In contrast, the DO_3 specimens exhibit high initial strain-hardening rates that gradually decrease to about the level of the B2 specimens. The 2% Cr samples had higher strain-hardening rates than the 5% Cr samples for each ordered condition. It is interesting to note that although a number of modified Hollomon empirical equations commonly used to describe experimental flow curves fit the tensile data of these specimens well [18–20] (correlation coefficients, r^2, were generally greater than 0.99), the constants obtained were not useful for quantifying trends observed by inspecting the flow curves [21].

Fig. 11 shows the flow curves for three 2% Cr sheet specimens heat treated to result in varying amounts of DO_3 order. The differences in flow stress reflect differing strain-hardening behaviour. The sample oil quenched directly from 700 °C is expected to have no DO_3 order, based on XRD results of other similarly heat-treated specimens. This condition resulted in the least strength, least strain hardening and greatest ductility of the three specimens. The specimen held at 400 °C for 24 h before oil quenching has the highest strength and strain hardening and the least ductility, while the specimen held at 500 °C for 24 h has intermediate strength, strain hardening and ductility. Although both ageing temperatures are below the critical temperature where DO_3 forms, the equilibrium degree of order decreases as the critical temperature is approached [10], so that the specimen held at 400 °C is expected to have the most DO_3 order although the kinetics of the $B2 \leftrightharpoons DO_3$ transformation are slower at the lower temperature. The order parameters of the two DO_3 ordered specimens are presented in Table III. Binary Fe_3Al of comparable grain size tested in compression has shown a similar effect [22] with the strain hardening, defined as $(\sigma_{4\%} - \sigma_{2\%})/2$, increasing with higher DO_3 order parameters. Strain-hardening values for the specimens described above are significantly higher than those reported in the literature for binary Fe_3Al [22], particularly those with the most DO_3 order, indicating that chromium additions may contribute to strain hardening as well as to increased yield strength in these alloys.

4. Conclusion

Fe_3Al alloyed with 2% Cr has somewhat higher yield strength than that with 5% Cr, but similar ductility. More highly ordered material has higher strength and, because higher order parameters are measured in the 2% Cr alloy, it appears that chromium inhibits ordering. The $B2 \leftrightharpoons DO_3$ reaction is quite sluggish in chromium-containing iron aluminide and can easily be suppressed to form only B2 order by oil quenching.

Better room temperature ductilities result from B2 order; however, this heat treatment is not suitable for applications where elevated temperatures of about 550 °C and above are anticipated, because the B2 structure is metastable and a transformation to DO_3 order will eventually occur. The DO_3 ordered structure generally results in higher flow stress than the B2 structure because of its higher strain-hardening rate, particularly when very few dislocations are present, although the DO_3 yield strength is actually lower

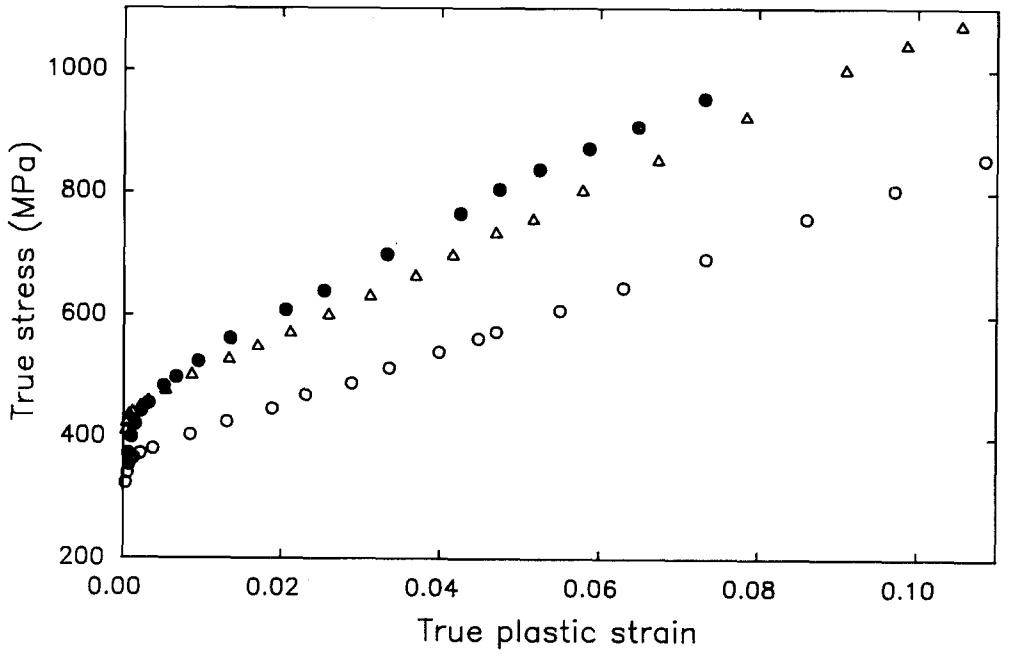

Figure 11 Flow curves for 2% Cr alloy sheet specimens with varying amounts of DO_3 order. (●) 2h, 700 °C, FG to 400 °C, hold 24 h. (△) 2 h, 700 °C, FC to 500 °C, hold 24 h. (○) 2 h, 700 °C, OQ.

when all dislocations have been eliminated by annealing.

Prior work improves both strength and ductility in these alloys. The optimum room-temperature properties can be obtained by heat treating to produce B2 order after warm working to generate a defect structure in a fine-grained material, provided the dislocation density is not sufficient to result in significant recrystallization during the ordering heat treatment. Room-temperature ductilities of 15%–20% result, although the fracture mode remains primarily brittle cleavage.

Acknowledgements

This work was supported by the US Department of Energy, Office of Fossil Energy. The portion of the work done at the INEL was under DOE contract no. DE-AC07-76IDO1570, and the portion of the work done at the ORNL was under DOE contract no. DE-AC05-840R21400 with Martin Marietta Energy Systems. The authors gratefully acknowledge the assistance of M. D. Harper, G. L. Fletcher, A. W. Erickson, V. L. Smith-Wackerle.

References

1. M. JOHNSON, D. E. MIKKOLA, P. A. MARCH and R. N. WRIGHT, *Wear* **140** (1990) 279
2. C. T. LIU, E. H. LEE and C. G. McKAMEY, *Scripta Metall.* **23** (1989) 875.
3. *Idem, ibid.* **24** (1990) 385.
4. C. T. LIU and E. P. GEORGE, *ibid.* **24** (1990) 1285.
5. D. B. KASUL and L. A. HELDT, *ibid.* **25** (1991) 1047.
6. D. J. GAYDOSH and M. V. NATHAL, *ibid.* **24** (1990) 1281.
7. C. G. McKAMEY, J. A. HORTON and C. T. LIU, *J. Mater. Res.* **4** (1989) 1156.
8. *Idem, Scripta Metall.* **22** (1988) 1679.
9. V. K. SIKKA, C. G. McKAMEY, C. R. HOWELL and R. H. BALDWIN, in "Fabrication and Mechanical Properties of Fe_3Al-Based Iron Aluminides" ORNL/TM-11465, Oak Ridge, TN, March 1990.
10. R. T. FORTNUM and D. E. MIKKOLA, *Mater. Sci. Engng* **91** (1987) 223.
11. R. S. DIEHM and D. E. MIKKOLA, in "Materials Research Society Symposium Proceedings on High Temperature Ordered Intermetallic Alloys", Vol. 81 (Materials Research Society, New York, 1987) p. 329.
12. R. S. DIEHM, M. P. KEMPPAINEN and D. E. MIKKOLA, *Mater. Manuf. Proc.* **4** (1989) 61.
13. L. ANTHONY and B. FULTZ, *J. Mater. Res.* **4** (1989) 1140.
14. K. OKI, M. HASAKA and T. EGUCHI, *Trans. JIM* **15** (1974) 143.
15. J. E. KRZANOWSKI and S. M. ALLEN, *Acta Metall.* **31** (1983) 213.
16. M. G. MENDIRATTA, S. K. EHLERS, D. K. CHATTERJEE and H. A. LIPSITT *Metall. Trans.* **18A** (1987) 283.
17. V. K. SIKKA, R. H. BALDWIN, C. R. HOWELL and J. H. REINSHAGEN, in "1990 Advances in Powder Metallurgy", edited by E. R. Andreotti and P. J. McGeehan (Metal Powder Industries Federation Proceedings 2, Princeton, NJ, 1990) p. 207.
18. P. LUDWIK, "Elemente der Technologischen Mechanik" (Springer, Berlin, 1909) p. 32.
19. H. W. SWIFT, *J. Mech. Phys. Solids* **1** (1952) 1.
20. D. C. LUDWIGSON, *Metall. Trans.* **2** (1971) 2825.
21. A. W. BOWEN and P. G. PARTRIDGE, *J. Phys. D Appl. Phys.* 7 (1974) 969.
22. R. G. DAVIES and N. S. STOLOFF, *Acta Metall.* **11** (1963) 1187.

Received 12 August 1991
and accepted 7 May 1992